Neurochemical Research (2019) 44:1715–1725
https://doi.org/10.1007/s11064-019-02802-8

ORIGINAL PAPER

Quercetin and Sodium Butyrate Synergistically Increase Apoptosis in Rat C6 and Human T98G Glioblastoma Cells Through Inhibition of Autophagy

Matthew A. Taylor[1] · Firas Khathayer[1] · Swapan K. Ray[1]

Received: 18 February 2019 / Revised: 10 April 2019 / Accepted: 11 April 2019 / Published online: 22 April 2019
© Springer Science+Business Media, LLC, part of Springer Nature 2019

Abstract

This study investigated the efficacy of quercetin (QCT) in combination with sodium butyrate (NaB) in enhancing apoptosis in rat C6 and human T98G glioblastoma cells though blockage of autophagy under nutrient-starvation. The most synergistic doses of the drugs were determined to be 25 μM QCT and 1 mM NaB in both cell lines. After QCT and QCT + NaB treatments, autophagy quantification with acridine orange staining showed a drastic decrease in protective autophagy in the cells under nutrient-starvation. Decrease in autophagy was correlated with decreases in expression of Beclin-1 and LC3B II. Combination treatment increased the morphological signs of apoptosis including membrane blebbing, nuclear fragmentation, and chromatin condensation. Annexin V staining was also performed for detection and quantification of increases in apoptosis. Western blotting results showed that combination of QCT and NaB increased apoptosis by decreasing anti-apoptotic Bcl-2 and increasing pro-apoptotic Bax, decreasing survivin, activating caspase-3, and degrading poly (ADP-ribose) polymerase (PARP). This study demonstrated the therapeutic potentials of a novel combination therapy in inhibiting protective autophagy to enhance apoptosis in rat C6 and human T98G glioblastoma cells.

Keywords Apoptosis · Autophagy · Glioblastoma · Quercetin · Sodium butyrate · Synergism

Introduction

Glioblastoma multiforme, commonly called glioblastoma, is the most prevalent and aggressive primary brain tumor in adults. With a 5-year survival rate of approximately 11.5%, glioblastoma remains one of the most difficult tumors to treat successfully [1]. This is due to the diffuse nature and progressive growth of many glioblastomas; many tumor cells infiltrating into crucial regions of the brain with ill-defined borders. Many glioblastomas also become resistant to the standard chemotherapy drug Temozolomide (TMZ) due to activation of MGMT (O^6 methylguanine-DNA methyltransferase) enzyme. This counteracts the tumor cell killing effects of TMZ and compromising therapeutic efficacy of TMZ leads to an average survival time of 14.6 months only from the time of diagnosis [2]. A substantial amount of research has been conducted in developing alternative glioblastoma therapies; however, few have been successful [3]. The vast complexity of the disease and current shortcomings of modern treatments highlight the need for continued investigation to find novel and alternative therapies that can extend the lives of many glioblastoma patients.

Quercetin (QCT) is one of the most abundant naturally occurring flavonoids, most commonly found in foods such as onions, red kidney beans, and tomatoes. For centuries, QCT has been well-established as a compound with vast therapeutic benefits. Most widely known for its anti-inflammatory properties, QCT has recently been shown to possess powerful anti-tumor effects in a wide variety of cancers, including glioblastoma [4]. In vivo concentrations in the micromolar (μM) range promote apoptosis in glioblastoma through inactivation of heat-shock protein (HSP)-27 and HSP-72 [5], activation of caspase-3 and caspase-9 [6], and inhibition of the mitogen-activated protein kinase (MAPK) pathway [7]. But despite the powerful anti-tumor properties of QCT, its inadequate bioavailability in vivo make it

✉ Swapan K. Ray
swapan.ray@uscmed.sc.edu

[1] Department of Pathology, Microbiology, and Immunology, University of South Carolina School of Medicine, 6439 Garners Ferry Road, Columbia, SC 29209, USA

a suitable candidate for pairing with previously established cancer therapies for synergistic therapeutic effects.

Sodium butyrate (NaB) is a histone deacetylase inhibitor (HDACi) that has been shown to exert anti-tumor effects in prostate, colon, breast, and hepatic tumors. In general, preclinical studies have shown that many HDACi compounds contain therapeutic potential in glioblastoma [8]. However, little is known about the therapeutic benefits of NaB, specifically, in glioblastoma. A recent study demonstrated that NaB inhibited glioblastoma invasion and induced senescence in vitro, but the exact mechanism is still unknown [9]. HDACi compounds act by inhibiting the HDAC enzymes, which remove acetyl groups from histone lysine residues; thereby allowing DNA to tightly coil and prevent transcription of various tumor suppressor genes. Many cancers have HDAC overexpression, and by inhibiting the HDAC enzymes, transcription of the previously silenced tumor suppressor genes may make allowance for suppression of tumor growth [10].

Autophagy is the evolutionarily conserved catabolic lysosomal degradation process that allows the tumor cells to quickly adapt and survive in hostile environments such as hypoxia, nutrient-starvation, and various cancer treatments; this is also known as 'protective autophagy' [11]. In cancer therapy, the exact role of autophagy remains a controversial topic without a clear answer [12]. On one hand, it has been shown that inhibition of protective autophagy in cell populations already exposed to a stressful environment can enhance cancer therapies and promote increased levels of apoptosis [13]. On the other hand, prolonged autophagy has also been shown to promote autophagic cell death, also known as type II programmed cell death. This has been proven to be beneficial in radiation therapy as well as in cell populations demonstrating resistance to apoptosis [14]. This study is demonstrating how protective autophagy inhibition in rat and human glioblastoma cells undergoing nutrient-starvation lowers tumor cell's natural defense mechanism and enhances potential of a novel combination therapy in two different glioblastoma cell lines.

Materials and Methods

Reagents

Hyclone™ RPMI-1640 Medium, Hyclone™ trypsin–EDTA, phosphate-buffered saline (PBS, Fisher Scientific), fetal bovine serum (BioABChem), penicillin/streptomycin (Cellgro®), 0.4% trypan blue solution (Sigma Aldrich), Kwik-Diff™ Solution #1, Kwik-Diff™ Solution #2, Kwik-Diff™ Solution #3, acridine orange (Invitrogen™), Annexin V-FITC (BD Biosciences), propidium iodide (BD Biosciences), Annexin V buffer solution (BD Biosciences), caspase-3 polyclonal antibody (Santa Cruz Biotechnology), LC3B monoclonal antibody (Cell Signaling Technologies), Poly (ADP-ribose) polymerase (PARP) monoclonal antibody (Cell Signaling Technologies), survivin monoclonal antibody (Santa Cruz Biotechnology), Bcl-2 polyclonal antibody (Santa Cruz Biotechnology), Bax polyclonal antibody (Santa Cruz Biotechnology), β-Actin polyclonal antibody (Santa Cruz Biotechnology), Beclin-1 (Santa Cruz Biotechnology) 4× Laemmli Sample Buffer (Bio-Rad), Clarity™ Western ECL Substrate (Bio-Rad), quercetin (Sigma Aldrich), and sodium butyrate (Sigma Aldrich).

Cell Culture and Treatments

Rat C6 and human T98G glioblastoma cells were obtained from the American Type Culture Collection (ATCC, Manassas, VA, USA). All cell lines were grown in Hyclone™ RPMI-1640 medium with 10% fetal bovine serum (FBS) and 1% penicillin/streptomycin (P/S). For serum-starvation, cells were grown in Hyclone™ RPMI-1640 medium with 0% fetal bovine serum (FBS) and 1% P/S. Cells were grown in a fully-humidified incubator at 37 °C with 5% CO_2. Appropriate amounts of glioblastoma cells were plated on either 100 × 15 mm petri dishes or 6-well suspension culture plates according to each experimental protocol. Cells were grown for 24 h in RPMI-1640 medium containing 10% FBS and 1% P/S for 24 h to allow cell adhesion and recovery to occur. Cells were then serum-starved for 24 h with RPMI-1640 medium containing 0% FBS and 1% P/S for 24 h in order to induce autophagy. Cells were then treated for 24 h with either 25 μM QCT, 1 mM NaB, or a combination of 25 μM QCT and 1 mM NaB. Control cells were grown in replenished serum-starved medium (RPMI-1640 with 0% FBS and 1% P/S). Cells were then tested with the appropriate experimental protocols.

Trypan Blue Dye Exclusion Assay

Both C6 and T98G cell lines were plated on Corning® 24-well flat-bottom plates and grown until confluency. The cells were then serum-starved using RPMI-1640 medium, 0% FBS, and 1% (P/S) for 24 h. Appropriate QCT and NaB concentrations were achieved through serial dilution with the serum-starved medium. Cells were treated with the designated drug combinations for 24 h. Cells were harvested via trypsinization, followed by two washes with 1× phosphate-buffered saline (PBS), and finally suspended in 1× PBS. One part cell suspension was mixed with one part 0.4% Trypan Blue solution for 3–5 min at room temperature. The cells were counted on a hemocytometer at 10× magnification using an Olympus BX53 microscope (Olympus America).

Viability was determined by assessing membrane permeability. Dead or dying cells develop a permeable membrane.

Cells stained with trypan blue were considered inviable due to their lack of membrane integrity. However, the trypan blue exclusion assay is not without its downfalls. Firstly, it assumes that all apoptotic cells have a permeable membrane, which is not always the case [15]. The test also relies on manual quantification of apoptotic cells by the experimenter. Human error may cause variability in the data. But despite these downfalls, the trypan blue exclusion assay is believed to be a sufficient test to calculate synergism between various QCT and NaB doses.

Determination of Decrease in Cell Viability and Synergism via Trypan Blue Dye Exclusion Assay

Cell viability was calculated with the equation: *Viable cells (%) = 100 − (number of dead cells ÷ total cells) × 100*. All experiments were performed in triplicate using approximately 300 cells per sample. The cell viability was then input into the program CompuSyn (ComboSyn, Paramus, NJ) to calculate combination index (CI) value. CompuSyn bases its calculations on the median-effect equation. Developed by Paul Talalay and Ting-Chao Chou in 1984, the median-effect equation combines the Hill equation, Henderson-Hasselbalch, Michaelis–Menten, and Scatchard equations to provide a normalization equation that aims to quantify synergism. CI value closest to 0 indicates the most synergistic action. CI values greater than 1 indicate antagonistic drugs, and a CI value of 1 indicates purely additive effects [16].

Acridine Orange Staining Using Fluorescent Microscopy to Determine Levels of Autophagy

Acridine orange (AO) staining is a versatile approach to analyzing variations in the cell cycle. With autophagy, AO staining visualizes the occurrence of the acidic vesicular organelles (AVOs) that are a classic sign of hallmark autophagic lysosomal degradation process. Acridine orange readily penetrates cell membranes and then remains inside the cell due to the low pH [17]. To visualize the response of AVO formation in response to treatment, approximately 1×10^6 cells were plated onto coverslips inside Corning® 6-well plates and grown for 24 h. Cells were then serum-starved and treated with QCT, NaB, or QCT + NaB as per the previously mentioned experimental protocol. Cells were then washed twice with 1× PBS followed by adding 1 ml of 1 µg/ml AO dye to each well and incubated for 15 min at 37 °C. The coverslips were then removed and read with a Leica™ 2500 fluorescent microscope using a Texas Red filter at 40× magnification. AVO formation appeared as a bright red fluorescence.

Acridine Orange Staining and Flow Cytometry to Determine Levels of Autophagy

Afterwards, the samples were analyzed using a BC FC500 Flow Cytometer by measuring the FL-3 intensity, which directly correlated to the amount of AVO formation [18, 19]. Cells were grown using the previously mentioned procedure. At the time of collection, the cells were collected into 1.5-ml microcentrifuge tubes and centrifuged at 3000 rpm for 4 min. The cells were incubated with 200 µl of 1 µg/ml AO dye for 15 min. The AO dye was then removed and replaced with 500 ml 1× Annexin V binding buffer. Inside the flow cytometer, the FL-3 channel was measured to correlate the amount of AVO present. Since all cells undergo a small amount of autophagy for homeostatic maintenance, a baseline level must be determined [20]. As a result, all samples were normalized using FL-3 measurements from samples not undergoing serum-starvation. This means that, for experimental purposes, all cells grown in ideal growing conditions were considered to have 0% autophagy. All treatments were performed in triplicate and used to form a mean.

Wright Staining for Morphological Signs of Apoptosis

Approximately 100,000 to 300,000 cells were grown in Corning® 6-well plates for 24 h. Upon adherence, the cells were serum-starved for 24 h using RPMI-1640 medium, 0% FBS, and 1% P/S to induce autophagy. Samples were then treated with QCT 25 µM, NaB 1 mM, or QCT + NaB for 24 h. Wright Staining was performed using the Kwik-Diff™ staining kit per the manufacturer's protocol. After the addition and incubation of Solutions # 1 to 3, samples were washed with 1 ml dH_2O to remove any excess dye not bound to cells. Samples were then read at 10× magnification using an Olympus BX53 microscope. Images were taken using an Olympus SC30 camera. Apoptosis quantification was performed under the criteria that apoptotic cells contained 1 or more of the following morphological signs: (1) crescent shaped nucleus, (2) nuclear condensation, (3) cell shrinkage, and (4) nuclear fragmentation. Necrotic cells were negligible and not included in the calculations.

Annexin V/Propidium Iodide (PI) Staining for Determining Apoptosis

The Annexin V/PI test is one of the most common methods for accurate and precise detection of apoptosis. The Annexin V is a Ca^{2+} dependent phospholipid binding protein that binds to externalized phosphatidylserine, which occurs during the early stages of apoptosis. PI is a fluorescent dye that is unable to penetrate intact cell membranes. When membrane integrity is lost due to necrosis or mechanical damage, PI penetrates the

membrane and signals that the damage has occurred. Mechanically damaged cells appear in quadrant A1, A2 represents necrotic cells, A3 contains viable cells, and A4 represents the amount of apoptotic cells in the population. The cells were grown and treated by using the previously described experimental protocol. Approximately 500,000 cells were grown and treated in Corning® 6-well plates, then harvested and stained according to the BD Biosciences standard Annexin V protocol. The samples were then read using a BC FC500 Flow Cytometer and displayed on a biaxial graph. Annexin V^+ cells were represented on the X-axis while PI^+ cells were represented on the Y-axis. The approximate percentage of apoptotic cells were displayed in quadrant A4, indicating Annexin V^+/PI^- cells.

Western Blotting

Western blotting was performed to examine changes in the expression of various apoptotic and autophagic proteins. Cells were grown and treated according to the previously described experimental protocol. The cells were then harvested via scraping and suspended in a 200 µl RIPA (radio-immunoprecipitation assay) lysis buffer + β-mercaptoethanol solution and stored at −20 °C for no-longer than 6 months. SDS-PAGE (sodium dodecyl sulfate-polyacrylamide gel electrophoresis) was performed on 4–20% Mini-Protean TGX Precast Gels purchased from Bio-Rad. The proteins were then transferred onto PVDF (polyvinyl difluoride) Transfer Membrane (Thermo Scientific). Then the membranes were blocked with 1× PBST (PBS supplemented with Tween 20) + 5% non-fat milk for 1 h to reduce non-specific binding of antibody. The membranes were then probed with a primary antibody at 4 °C overnight, washed with PBST, and then probed with the corresponding secondary antibody for 30 min at room temperature. They were then exposed and analyzed using ImageJ software (National Institutes of Health, USA).

Statistical Analysis

Statistical analyses were performed using Minitab Express software. Data were presented as a mean + standard error of mean (SEM) of independent experiments ($n \geq 3$). Comparisons calculated by One-Way ANOVA (analysis of variance) using the Tukey Method. Significant difference from control value is represented by $*p < 0.05$, $**p < 0.0001$.

Results

Determination of Synergism of QCT and NaB in C6 and T98G Cells

Trypan blue staining was performed to measure the amount of cell death after treatment with various doses of the drug combinations. The QCT concentrations 12.5, 25, 50, and 100 µM were used in combination with the NaB concentrations 1, 3, 5, and 8 mM, respectively, to see which combination had the most synergism for growth inhibition (Fig. 1). QCT caused the greatest amount of apoptosis in a dose dependent manner, while NaB appeared to cause negligible amounts of apoptosis in both cell populations. However, in combination, the drugs appeared to be acting in a synergistic manner to cause apoptosis. The synergism was confirmed using the median-effect equation. The drug combination with the lowest CI value indicated the highest amount of synergism, which was achieved with 25 µM QCT + 1 mM NaB in both rat C6 and human T98G glioblastoma cells (Table 1).

Examination of Morphological Features and Molecular Markers of Autophagy in Glioblastoma Cells

AO staining was used to quantify the change in autophagy following treatments. Fluorescent microscopy was used to visualize the high amounts of autophagy under the 48-h serum-starved control condition and the subsequent decrease in autophagy due to treatments with QCT and QCT + NaB (Fig. 2a). QCT was the primary autophagy inhibitor in both rat and human glioblastoma cells. NaB showed little effect on inhibiting or activating autophagy when compared with the control cells (Fig. 2b). By visualization of AVO formation, autophagy appeared to be reduced to baseline homeostatic levels in the human T98G cells under QCT + NaB treatment while under 48-h serum-starvation, as seen in Fig. 2a and b. Combination treatment caused a drastic decrease in autophagy in both the rat C6 and human T98G glioblastoma cells. Western blotting showed the changes in expression of molecules related to the induction of autophagy (Fig. 3a). Compared with QCT alone, there were 43% and 41% decreases in Beclin-1 expression (Fig. 3b), and 70% and 76% decreases in LC3B II expression with QCT + NaB treatment in C6 and T98G cells, respectively (Fig. 3c).

Determination of Morphological Features of Apoptosis in Glioblastoma Cells

Wright staining was used to visualize the morphological signs of apoptosis in rat C6 and human T98G cells in 48-h serum-starved and untreated conditions and after QCT, NaB, and QCT + NaB treatments (Fig. 4a). Characterization of apoptosis under the light microscopy was based on visual signs such as membrane blebbing, chromatin condensation, and nuclear fragmentation. Red arrows demonstrated cells to be considered apoptotic (Fig. 4a). These results were then quantified and displayed (Fig. 4b). The results showed

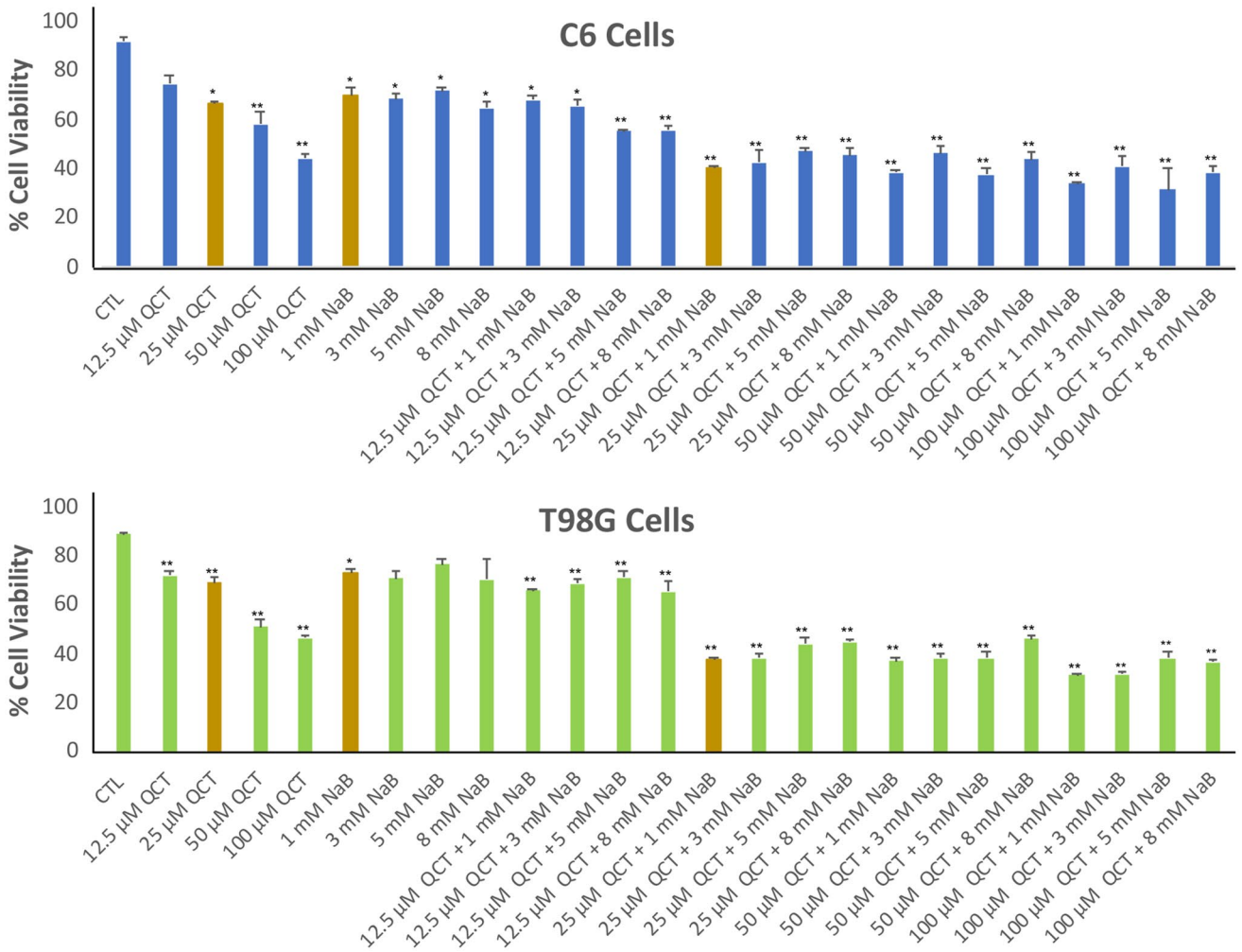

Fig. 1 Changes in cell viability in rat C6 and human T98G glioblastoma cells after treatments with QCT, NaB, and QCT + NaB. Untreated cells under 48-h serum-starvation were used as a control. The highlighted bars are indicating the most synergistic drug combination according to the median-effect equation

26.7% and 27.2% apoptosis in C6 and T98G cells, respectively, with single QCT treatment (Fig. 4b). With single NaB treatment, C6 and T98G had 24.0% and 25.4% apoptosis, respectively. QCT + NaB treatment showed 49.2% and 51.06% apoptosis in C6 and T98G cells, respectively. Compared with the single QCT treatment, QCT + NaB treatment yielded 84.3% and 87.7% apoptosis in C6 and T98G cells, respectively. These results indicated that QCT and NaB were acting synergistically with each other to increase apoptosis in C6 and T98G cells under serum-starvation.

Determination of a Biochemical Feature of Apoptosis in Glioblastoma Cells

Annexin V/PI staining was used to quantify apoptotic cells versus necrotic cells (Fig. 5a). QCT treatment in both rat C6 and human T98G cells showed 32.2% and 36.1% apoptosis (Fig. 5b). NaB treatment showed 22.0% and 28.7% apoptosis in C6 and T98G cells, respectively. Treatment with QCT + NaB showed 39.5% and 43.0% apoptosis in C6 and T98G cells, respectively. Negligible amounts of necrosis were observed (quadrant A2), and mechanical damage was avoided (quadrant A1). These results directly correlated with the autophagy inhibition seen with AO staining. Human T98G cells demonstrated a complete suppression of autophagy due to QCT + NaB treatment, resulting in a 19.1% increase of apoptosis when compared with the QCT-only treated cells, which did not show complete suppression of autophagy. This indicated that autophagy might be playing a protective role in serum-starved glioblastoma cells.

Table 1 Combination index (CI) of QCT and NaB in C6 and T98G cells

C6 cells			T98G cells		
QCT (μM)	NaB (mM)	CI value	QCT (μM)	NaB (mM)	CI value
12.5	1	0.735	12.5	1	0.539
12.5	3	0.616	12.5	3	0.678
12.5	5	0.24	12.5	5	0.839
12.5	8	0.248	12.5	8	0.528
25	1	**0.175**	25	1	**0.147**
25	3	0.206	25	3	0.155
25	5	0.281	25	5	0.229
25	8	0.253	25	8	0.245
50	1	0.314	50	1	0.28
50	3	0.533	50	3	0.309
50	5	0.302	50	5	0.309
50	8	0.451	50	8	0.538
100	1	0.461	100	1	0.374
100	3	0.736	100	3	0.374
100	5	0.384	100	5	0.621
100	8	0.63	100	8	0.539

The CI values shown in bold (Table 1) indicate the most synergism with QCT + NaB concentrations in C6 and T98G cells

Alterations in Molecular Components for Increasing Apoptosis

Western blotting was performed focusing on selected proteins from three main target pathways: (1) changes in levels of autophagy marker proteins Beclin-1 and LC3B (Fig. 3), (2) confirmation of the intrinsic apoptotic pathway through alterations in Bax and Bcl-2 expression (Fig. 6a, b), (3) apoptosis induction through caspase-3 activation along with changes in expression of potential apoptosis suppressor proteins survivin and PARP (Fig. 6a). The Bax:Bcl-2 ratio was calculated to show if the QCT + NaB treatment was inducing the intrinsic pathway of apoptosis. The control samples showed a ratio of < 1, meaning that the cells generally were not undergoing apoptosis. Upon QCT treatment, the human T98G glioblastoma cells showed a ratio of 2.32; whereas the rat C6 glioblastoma cells had a ratio of 1.20. The NaB treatment showed a ratio of < 1 in both rat and human glioblastoma cells. Under combination treatment, both rat and human glioblastoma cells had a positive ratio of approximately 2.40 and 4.06, respectively (Fig. 6b). Caspase-3 cleavage for its activation demonstrated the final phase in the execution of apoptosis. The rat glioblastoma cells showed a clear increase in caspase-3 activity in the QCT + NaB treatment, while the human glioblastoma cells showed a conspicuous increase in caspase-3 activity in both the QCT and QCT + NaB treatments. Survivin expression in both rat and human glioblastoma cells was drastically reduced with the QCT + NaB treatment. In the rat C6 cells, PARP was reduced in the QCT + NaB treatment, while PARP was reduced across QCT, NaB, and QCT + NaB treatments in the human T98G cells. Autophagy related proteins Beclin-1 and LC3B were also investigated. In both rat and human glioblastoma cells, Beclin-1 was reduced in combination treatments, and it was also reduced in QCT treatment in the human glioblastoma cells. LC3B cleavage also showed to be greatly decreased in both rat and human glioblastoma

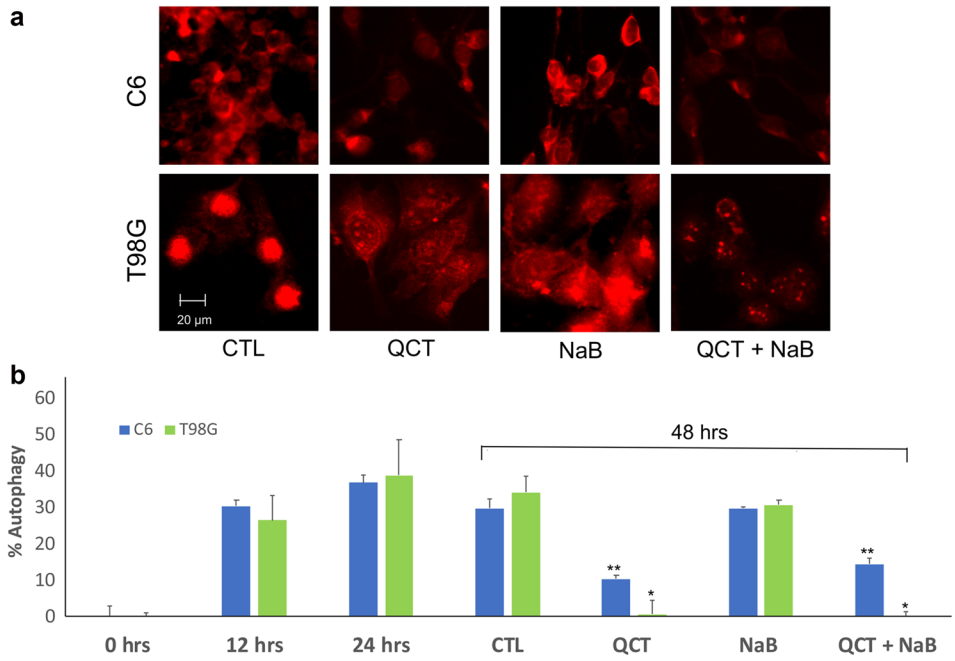

Fig. 2 Changes in autophagy in C6 and T98G cells after treatments. **a** Fluorescence microscopy showing AVO formation in rat C6 and human T98G cells. Red fluorescence is showing acidic autophagosomes that make up the key step in autophagy. **b** Flow cytometry data of FL-3 fluorescence density, indicating changes in autophagy (Color figure online)

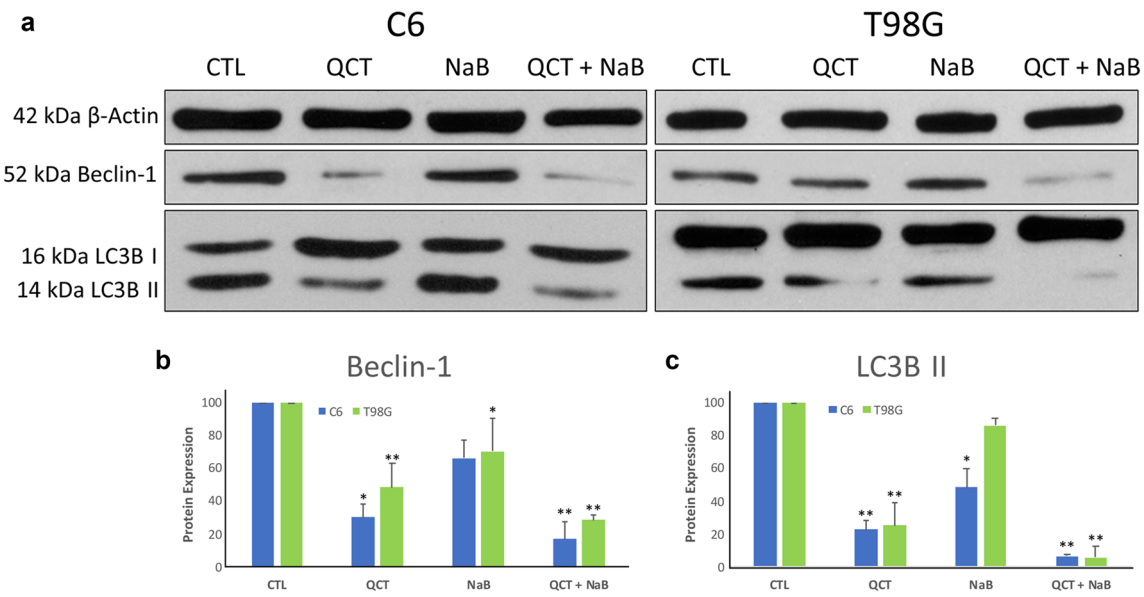

Fig. 3 **a** Western blotting for assessing changes in autophagy-related proteins such as Beclin-1 and LC3B. Both Beclin-1 and LC3B are pro-autophagy proteins. Therefore, their down regulation indicated targeted inhibition of autophagy at the molecular levels. **b** Western blot analysis of Beclin-1 protein expression. **c** Western blot analysis of LC3B II expression, both of which have a direct correlation with autophagy activation

cells in both QCT and QCT + NaB treatments. NaB alone did not have much impact on autophagy.

Discussion

The main aim of this study was to investigate the efficacy of a novel combination therapy in increasing apoptosis in rat and human glioblastoma cells though inhibition of protective autophagy. At this point, the idea of inhibiting protective autophagy or activating autophagic cell death is highly debated [11, 12]. One argument is that overactivation of autophagy will cause greater amounts of cell death in otherwise apoptosis-resistant cells. This type of therapy is seen with radiation treatment and some autophagy-inducing drugs like Itraconazole [21, 22]. The other argument is that by inhibiting protective autophagy, induced by many cancer therapies including TMZ, greater levels of apoptosis may be achieved [23].

The treatment of rat C6 and human T98G glioblastoma cells with synergistic combination of QCT and NaB demonstrated that amounts of apoptosis were increased with the inhibition of autophagy; thus, reinforcing the idea that inhibition of protective autophagy could prove beneficial to cancer therapy. It is interesting to note that in our experiments, QCT was deemed to be the primary autophagy inhibitor in both the rat and human glioblastoma cells as we demonstrated through the lack of AO staining and unseen cleavage of LC3B I to LC3B II. This directly contradicts a previous study performed on human U373MG glioblastoma cells showing that QCT activated autophagy, and that autophagy inhibition through Chloroquine potentiated its apoptotic effects [24]. This discrepancy may be due to the experimental conditions present in each study. Kim et al. did not seek to induce autophagy through nutrient-starvation before performing treatment [24]. Our study, however, was conducted in the nutrient-starved cells for 24 h before treating with QCT for another 24 h. This was done in order to mimic a tumor microenvironment, where many cells become autophagic due to high cell density causing an increased competition for nutrients [25]. This shows the capability of QCT to have opposite effects on autophagy depending on the environmental conditions. But both studies concluded that inhibition of autophagy potentiated the apoptosis-inducing effects of QCT in glioblastoma cells.

Combination of QCT with NaB, an HDACi, showed a synergistic increase in apoptosis in both rat and human glioblastoma cells. Presently, HDACi compounds are widely used in cancer therapies. For example, the HDACi Valproic Acid has been shown to be a radiosensitizer [26]. Presently, several studies have been done with NaB to show its impact on glioblastoma therapy. Our results showed that NaB alone did not induce high levels of apoptosis or had a substantial effect on autophagy. But when in combination with QCT,

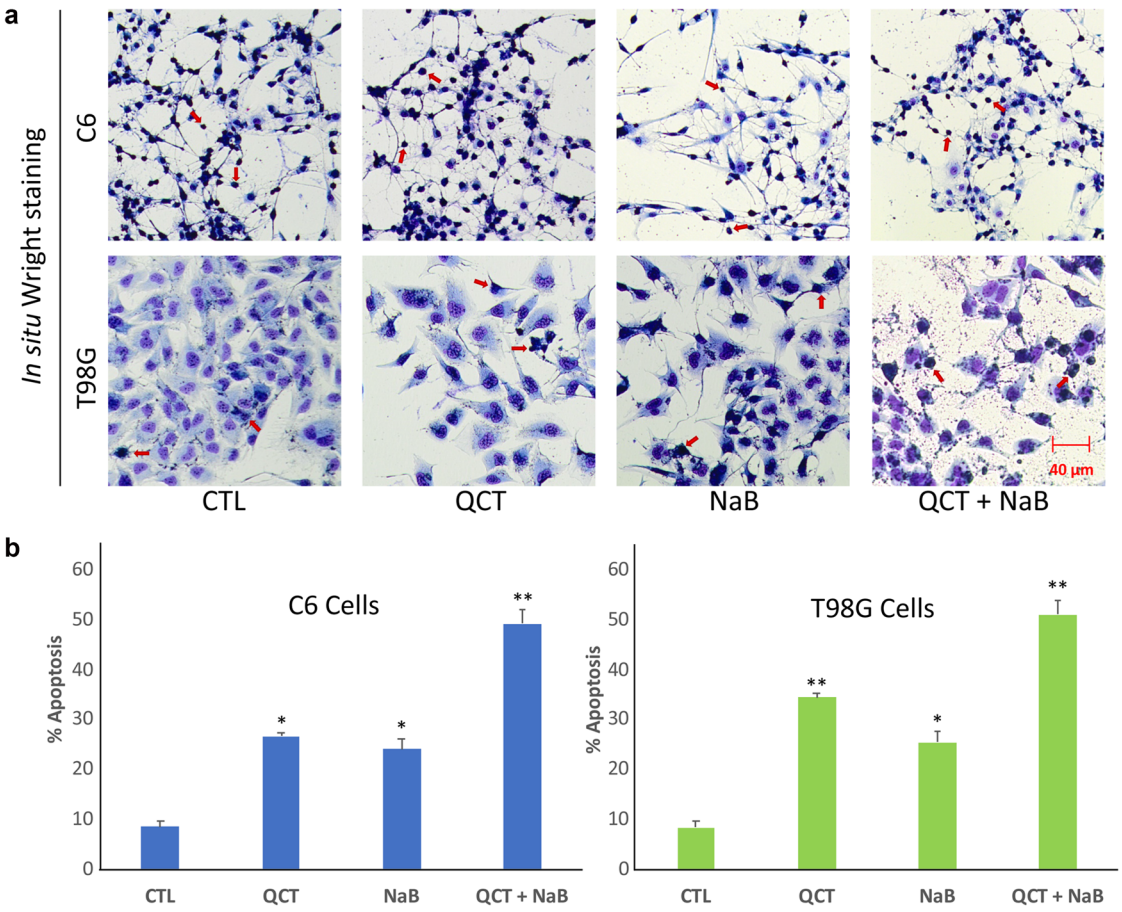

Fig. 4 Estimation of apoptosis based on morphological features. **a** Wright staining of C6 and T98G cells showing the morphological signs of apoptosis after treatments with QCT, NaB, and QCT + NaB during 48-h serum-starvation. **b** Apoptosis quantification based on the morphological markers of apoptosis

NaB synergistically decreased survivin expression in both rat and human glioblastoma cells, caused PARP degradation in the rat cells, and drastically increased caspase-3 activation as well in the rat glioblastoma cells. To our knowledge, this is the first demonstration of QCT + NaB acting synergistically in glioblastoma cells to induce apoptosis.

This study highlights two main ideas that are worth being further explored. Autophagy inhibition as a means to increase apoptotic cell death is a hotly debated topic whose benefits are still being uncovered. TMZ, the current first-line therapy for glioblastoma, is a proven autophagy inducing agent [27]. A common avenue utilizing TMZ is to overactivate the TMZ-induced autophagy to trigger autophagic cell death in apoptosis-resistant glioblastoma cells [28]. But it has also been widely proven that autophagy inhibition can increase radiosensitivity in glioblastoma [29] and increase cytotoxicity of TMZ in glioblastoma through increased PARP cleavage [30]. Knowing that tumor microenvironments promote autophagy through nutrient-starvation and that TMZ treatment further promotes autophagy, inhibiting the cell's protective mechanism makes intuitive sense for promoting increased cell death. Most studies targeting autophagy inhibition use Chloroquine due to its effectiveness in reducing autophagy. But Chloroquine is not an ideal candidate for cancer therapy in the clinics due to its common adverse side effects including cardiac disturbances, visual defects, and kidney damage [13]. This is why alternative autophagy inhibitors must be studied.

The second idea worth being explored is the use of alternative, less toxic therapies that promote autophagy inhibition. Flavonoids are metabolites found in many common foods. Recent research shows that certain flavonoids possess

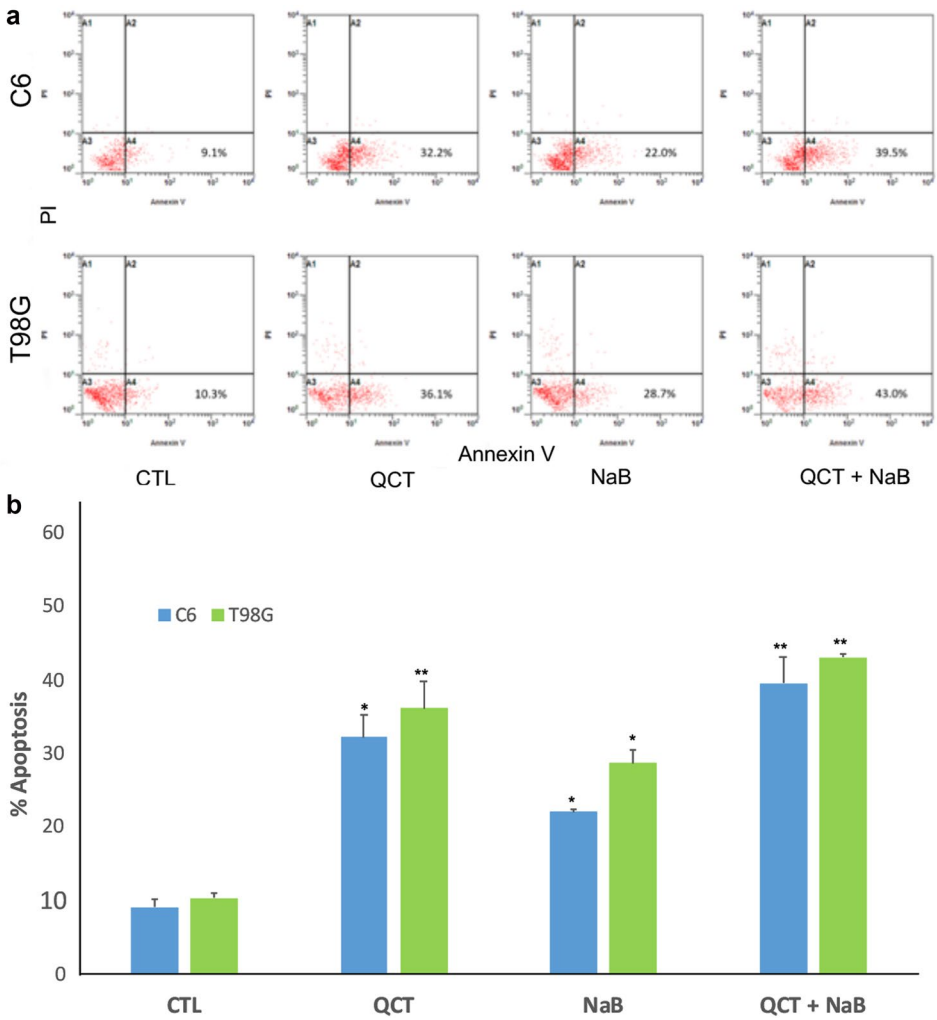

Fig. 5 Estimation of apoptosis based on a biochemical assay (Annexin V/PI staining). **a** Annexin V staining showing % apoptosis based on phosphatidylserine externalization in the A4 quadrant. **b** Average % apoptosis from Annexin V staining

potent anti-cancer effects [31]. For example, Luteolin, a naturally occurring flavonoid, successfully inhibited autophagy and increased apoptosis in two types of human glioblastoma cells [32]. QCT is another dietary flavonoid found in many common foods. We demonstrated in this study that QCT inhibited protective autophagy and increased apoptosis in both rat and human glioblastoma cells. Dietary flavonoids are becoming popular in the treatment of various cancers including glioblastoma in preclinical models. Because using a non-toxic flavonoid to inhibit protective autophagy provides a safer alternative avenue to using Chloroquine for autophagy inhibition [4]. Also, a flavonoid can be combined with another therapeutic agent for synergistic efficacy in inhibiting growth of cancers.

In conclusion, when used in combination, QCT and NaB in treating nutrient-starved rat and human glioblastoma cells inhibited protective autophagy and thereby increased apoptosis. This study demonstrated the therapeutic potential of inhibiting protective autophagy in a mimicked tumor microenvironment, while also providing insight into an alternative therapy for TMZ-resistant glioblastoma cells. Further investigations into the therapeutic benefits of QCT and protective autophagy inhibition are highly encouraged in rat allograft and human xenograft models of glioblastoma to establish efficacy of our novel combination therapy that may provide a way to increase the longevity in glioblastoma patients in the future.

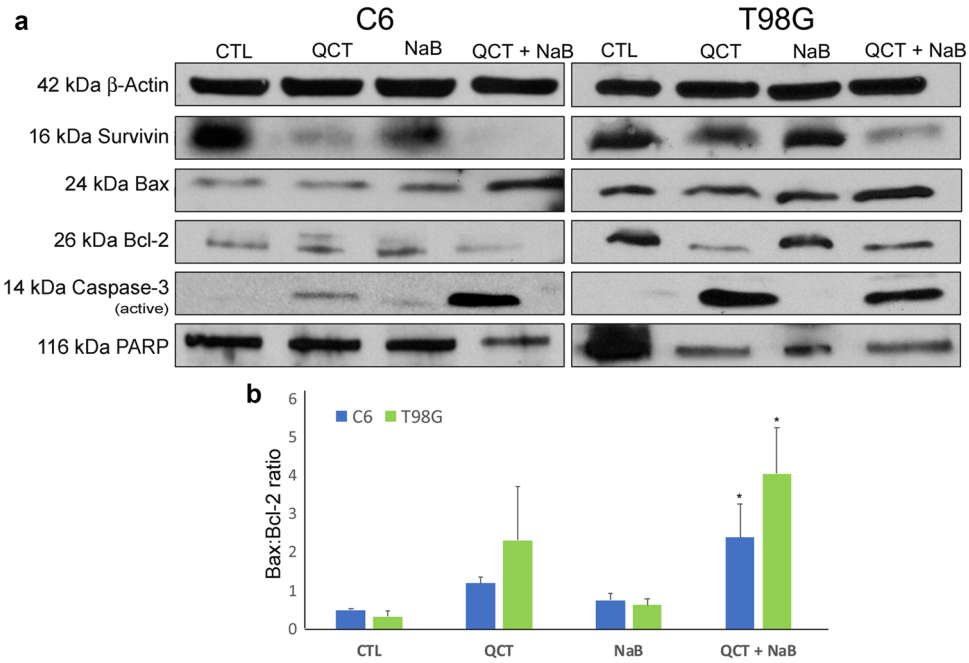

Fig. 6 **a** Western blotting showing changes in expression of various apoptosis-related proteins. Survivin, an anti-apoptotic protein, was down regulated due to the QCT + NaB treatment in both rat C6 and human T98G cells. Bax, a pro-apoptotic protein, was upregulated in both cell populations; while Bcl-2, an anti-apoptotic protein, was inhibited in both cell populations under QCT + NaB treatment. This indicated that apoptosis was occurring through the intrinsic pathway. Caspase-3, an essential protein in the downstream apoptosis pathway, was highly activated in both rat C6 and human T98G cell populations. PARP, a DNA repair protein, was inhibited only in QCT + NaB treatment in the rat C6 cells. In the human T98G cells, PARP was inhibited due to treatment with drug combination. **b** Graphical representation of the Bax:Bcl-2 ratio: values > 1 indicate that apoptosis is occurring through the intrinsic mitochondrial pathway

Acknowledgements This work was supported in part by an award from the Soy Health Research Program (SHRP, United Soybean Board, Chesterfield, MO, USA), a Grant (SCIRF-2015-I-0) from the Spinal Cord Injury Research Fund (SCIRF, Columbia, SC, USA), and also earlier R01 Grants (CA91460 and NS57811) from the National Institutes of Health (Bethesda, MD, USA).

Compliance with Ethical Standards

Conflict of interest The authors declare no conflict of interest.

References

1. Brodbelt A, Greenberg D, Winters T et al (2015) Glioblastoma in England: 2007–2011. Eur J Cancer 51:533–542. https://doi.org/10.1016/j.ejca.2014.12.014
2. Hottinger AF, Stupp R, Homicsko K (2014) Standards of care and novel approaches in the management of glioblastoma multiforme. Chin J Cancer 33:32–39. https://doi.org/10.5732/cjc.013.10207
3. Wang Y, Xing D, Zhao M et al (2016) The role of a single angiogenesis inhibitor in the treatment of recurrent glioblastoma multiforme: a meta-analysis and systematic review. PLoS ONE 11:1–13. https://doi.org/10.1371/journal.pone.0152170
4. Taylor M, Ray SK (2016) Prospects of enhancing anti-cancer activities of quercetin the treatment of glioblastoma. In: Watanabe H (ed) Horizons in cancer research. 2017 Nova Science Publishers Inc, New York, pp 173–192
5. Sang DP, Li RJ, Lan Q (2014) Quercetin sensitizes human glioblastoma cells to temozolomide in vitro via inhibition of Hsp27. Acta Pharmacol Sin 35:832–838. https://doi.org/10.1038/aps.2014.22
6. Bądziul D, Jakubowicz-Gil J, Langner E et al (2014) The effect of quercetin and imperatorin on programmed cell death induction in T98G cells in vitro. Pharmacol Rep 66:292–300. https://doi.org/10.1016/j.pharep.2013.10.003
7. Lee KW, Kang NJ, Heo Y-S et al (2008) Raf and MEK protein kinases are direct molecular targets for the chemopreventive effect of quercetin, a major flavonol in red wine. Cancer Res 68:946–955. https://doi.org/10.1158/0008-5472.CAN-07-3140
8. Yelton CJ, Ray SK (2018) Histone deacetylase enzymes and selective histone deacetylase inhibitors for antitumor effects and enhancement of antitumor immunity in glioblastoma. Neuroimmunol Neuroinflamm 5:46. https://doi.org/10.20517/2347-8659.2018.58
9. Nakagawa H, Sasagawa S, Itoh K (2018) Sodium butyrate induces senescence and inhibits the invasiveness of glioblastoma cells. Oncol Lett 15:1495–1502. https://doi.org/10.3892/ol.2017.7518
10. West AC, Johnstone RW (2014) New and emerging HDAC inhibitors for cancer treatment. J Clin Investig 124:30–39. https://doi.org/10.1172/JCI69738.30
11. Huang Z, Zhou L, Chen Z et al (2016) Stress management by autophagy: implications for chemoresistance. Int J Cancer 139:23–32. https://doi.org/10.1002/ijc.29990
12. Taylor MA, Das BC, Ray SK (2018) Targeting autophagy for combating chemoresistance and radioresistance in glioblastoma. Apoptosis 23:563–575. https://doi.org/10.1007/s10495-018-1480-9

13. Kimura T, Takabatake Y, Takahashi A, Isaka Y (2013) Chloroquine in cancer therapy: a double-edged sword of autophagy. Cancer Res 73:3–7. https://doi.org/10.1158/0008-5472.CAN-12-2464
14. Luca Gravina G, Mancini A, Mattei C (2017) Enhancement of radiosensitivity by the novel anticancer quinolone derivative vosaroxin in preclinical glioblastoma models. Oncotarget 8:29865–29886. https://doi.org/10.18632/oncotarget.16168
15. Cooper ST, McNeil PL (2015) Membrane repair: mechanisms and pathophysiology. Physiol Rev 95:1205–1240. https://doi.org/10.1152/physrev.00037.2014
16. Chou TC (2010) Drug combination studies and their synergy quantification using the chou-talalay method. Cancer Res 70:440–446. https://doi.org/10.1158/0008-5472.CAN-09-1947
17. Pierzynska-Mach A, Janowski PA, Dobrucki JW (2014) Evaluation of acridine orange, LysoTracker Red, and quinacrine as fluorescent probes for long-term tracking of acidic vesicles. Cytom Part A 85:729–737. https://doi.org/10.1002/cyto.a.22495
18. Kanzawa T, Zhang L, Xiao L et al (2005) Arsenic trioxide induces autophagic cell death in malignant glioma cells by upregulation of mitochondrial cell death protein BNIP3. Oncogene 24:980–991. https://doi.org/10.1038/sj.onc.1208095
19. Mohan N, Banik NL, Ray SK (2011) Combination of N-(4-hydroxyphenyl) retinamide and apigenin suppressed starvation-induced autophagy and promoted apoptosis in malignant neuroblastoma cells. Neurosci Lett 502:24–29. https://doi.org/10.1016/j.neulet.2011.07.016
20. Yang Z, Klionsky DJ (2010) Mammalian autophagy: core molecular machinery and signaling regulation. Curr Opin Cell Biol 22:124–131. https://doi.org/10.1016/j.ceb.2009.11.014
21. Liu R, Li J, Zhang T et al (2014) Itraconazole suppresses the growth of glioblastoma through induction of autophagy. Autophagy 10:1241–1255. https://doi.org/10.4161/auto.28912
22. Sharma K, Le N, Alotaibi M, Gewirtz DA (2014) Cytotoxic autophagy in cancer therapy. Int J Mol Sci 15:10034–10051. https://doi.org/10.3390/ijms150610034
23. Liu X, Sun K, Wang H, Dai Y (2016) Inhibition of autophagy by chloroquine enhances the antitumor efficacy of sorafenib in glioblastoma. Cell Mol Neurobiol 36:1197–1208. https://doi.org/10.1007/s10571-015-0318-z
24. Kim H, Moon JY, Ahn KS, Cho SK (2013) Quercetin induces mitochondrial mediated apoptosis and protective autophagy in human glioblastoma U373MG cells. Oxid Med Cell Longev 2013. https://doi.org/10.1155/2013/596496
25. White E (2015) The role for autophagy in cancer. J Clin Investig 125:42–46. https://doi.org/10.1172/JCI73941
26. Lee DH, Ryu H-W, Won H-R, Kwon SH (2017) Advances in epigenetic glioblastoma therapy. Oncotarget 8:18577–18589. https://doi.org/10.18632/oncotarget.14612
27. Yan Y, Xu Z, Dai S et al (2016) Targeting autophagy to sensitive glioma to temozolomide treatment. J Exp Clin Cancer Res 35:23. https://doi.org/10.1186/s13046-016-0303-5
28. Yu Q, Liu L, Wang P et al (2017) EMAP-II sensitize U87MG and glioma stem-like cells to temozolomide via induction of autophagy-mediated cell death and G2/M arrest. Cell Cycle. https://doi.org/10.1080/15384101.2017.1315492
29. Ye H, Chen M, Cao F et al (2016) Chloroquine, an autophagy inhibitor, potentiates the radiosensitivity of glioma initiating cells by inhibiting autophagy and activating apoptosis. BMC Neurol 16:178. https://doi.org/10.1186/s12883-016-0700-6
30. Golden EB, Cho H-Y, Jahanian A et al (2014) Chloroquine enhances temozolomide cytotoxicity in malignant gliomas by blocking autophagy. Neurosurg Focus 37:E12. https://doi.org/10.3171/2014.9.FOCUS14504
31. Li J, Wang Y, Lei JC et al (2014) Sensitisation of ovarian cancer cells to cisplatin by flavonoids from *Scutellaria barbata*. Nat Prod Res 28:683–689. https://doi.org/10.1080/14786419.2013.871547
32. Chakrabarti M, Ray SK (2016) Anti-tumor activities of luteolin and silibinin in glioblastoma cells: overexpression of miR-7-1-3p augmented luteolin and silibinin to inhibit autophagy and induce apoptosis in glioblastoma in vivo. Apoptosis 21:312–328. https://doi.org/10.1007/s10495-015-1198-x

Publisher's Note Springer Nature remains neutral with regard to jurisdictional claims in published maps and institutional affiliations.